Cellulose (2018) 25:3189–3196
https://doi.org/10.1007/s10570-018-1773-8

COMMUNICATION

# Highly flexible, transparent, and conductive silver nanowire-attached bacterial cellulose conductors

**Pengfei Lv · Huimin Zhou · Min Zhao · Dawei Li · Keyu Lu · Di Wang · Jieyu Huang · Yibing Cai · Lucian Amerigo Lucia · Qufu Wei**

Received: 29 December 2017 / Accepted: 2 April 2018 / Published online: 19 April 2018
© Springer Science+Business Media B.V., part of Springer Nature 2018

**Abstract** A simple, rapid method for developing conductive, ultrafine, and high aspect ratio silver nanowires (AgNWs) is reported. Transparent and flexible nanocomposites were fashioned from bacterial cellulose (BC) and AgNWs in a very straightforward and direct manner without the addition of materials or the need for specific facilities. The as-prepared BC/AgNWs composite thin films were able to demonstrate acceptable transparency (near 80% at 550 nm), high flexibility, good mechanical strength (18.95 MPa) and stable conductivity (7.46 $\Omega$ sq$^{-1}$) under various bending states.

**Keywords** Silver nanowires · Bacterial cellulose · Transparency · Flexibility · Thin films · Mechanical strength

P. Lv · H. Zhou · M. Zhao · D. Li · D. Wang · J. Huang · Y. Cai · Q. Wei (✉)
Key Laboratory of Eco-Textiles, Jiangnan University, Wuxi 214122, China
e-mail: qfwei@jiangnan.edu.cn

K. Lu
State Key Laboratory of Food Science and Technology, Jiangnan University, 1800 Lihu Avenue, Wuxi 214122, Jiangsu, People's Republic of China

L. A. Lucia (✉)
Fiber and Polymer Science, North Carolina State University, 2401 Research Drive, Campus Box 8301, Raleigh, NC 27695-8301, USA
e-mail: lalucia@ncsu.edu

## Introduction

Recently, flexible and stretchable electrodes have elicited significant attention due to their intrinsically fascinating properties that include adaptability under a variety of conditions, light weight, and potential for high functionality. They have found great utility as optoelectronic devices artificial skin, stretchable displays, solar cells, touch screens, and light-emitting diodes (LEDs) (Ellmer 2012; Liu et al. 2017; Sekitani et al. 2009). One of the leading and most applied electrodes for transparent conducting applications is indium thin oxide (ITO) because of its high optical transmittance (> 90% at 550 nm) and excellent electrical conductivity (10–20 $\Omega$ sq$^{-1}$). However, ITO suffers from serious drawbacks such as brittleness, high cost, hard-fabrication process and inherent processing difficulties, all of which further limits its industrial application as a flexible electrode (Kim et al. 2013). To date, ITO is now being gradually substituted with flexible transparent materials, such as conducting polymers, carbon-based materials and metallic (copper or silver) nanowires (NWs) (Bobinger et al. 2017; Dong et al. 2018; Hecht et al. 2011; Lin et al. 2013; Lu et al. 2017; Zhang et al. 2017). Among them, silver nanowires (AgNWs) have been a leading candidate because of their good mechanical properties, efficient electrical performances, high transmittance, easy large-scale preparation and facile deposition on various types of substrates (Bade et al. 2016; Celle et al. 2012; Wu et al. 2016; Zeng et al. 2010). Despite the

significant benefits of AgNWs for developing transparent conducting materials, to date few transparent and flexible devices based on AgNWs have been reported.

Bacterial cellulose (BC) is a biomaterial synthesized by vinegar bacteria, such as *Komagataeibacterxylinus* (*K. xylinus*) (ATCC 10245). It is a low-cost and eco-friendly biomacromolecule that in relation to its analogous plant-based fibers, has many advantages including high mechanical strength (200–300 MPa), excellent flexibility, and very high biocompatibility (Ramani and Sastry 2014; Thiruvengadam and Vitta 2017). Hence, it has been widely used in many areas such as biomedicine (Qiu et al. 2016; Schumann et al. 2009), foods (Fabra et al. 2016; Ullah et al. 2016), flexible electrodes (Hu et al. 2011; Peng et al. 2016; Wang et al. 2013) and reinforced materials (Trovatti et al. 2013; Wu et al. 2018), etc. Meanwhile, BC has the unique ability to endow high optical capacity such as witnessed in the fabrication of transparent nanobiocomposites that possess excellent optical properties and flexibility (Pinto et al. 2015). Recently, Wu and Cheng (2016) reported highly transparency (83% at 550 nm) BC composite films that upon oxidation with 2,2,6,6-tetramethylpiperidine-1-oxyl radical (TEMPO) self-assemble.

In this work, a simple and rapid method for the preparation of highly conductive and stretchable AgNWs is reported. A new type of AgNWs nanocomposite transparent films based on a flexible BC matrix as the overcoating layer was fabricated via a rapid one-step method. This approach endows a flat surface highly stable conductivity, good mechanical strength, satisfactory transparency, easy ablation, and good resistance to organic and inorganic solvents.

## Experimental section

### Materials

The BC was self-made from in-house lab (Jiangnan University, China). The $AgNO_3$ was purchased from Sigma Aldrich (USA). Poly(*N*-vinyl-2-pyrrolidone) (PVP) (Molecular weight: 15,000), Ethanediol (EG) and $CuCl_2$ were obtained from Sinopharm Chemical Reagent. Co., Ltd. (China). Yeast extract, D-mannitol, Bacto peptone and NaOH of analytical grade were purchased from Aladdin Bio-Chem Technology Co., Ltd (Shanghai, China). All of the chemicals were of analytical grade and solutions were prepared with deionized water.

### Preparation of AgNWs-attached BC nanocomposites

BC pellicles were synthesized by a typical method as previously reported (Lv et al. 2017). The details of the synthesis procedure are described as follows: BC pellicles were produced by cultivating *K. Xylinus* in the classical Hestrin and Schramm (HS) medium that contained 5 g $L^{-1}$ yeast, 3 g $L^{-1}$ bacto-peptone and 25 g $L^{-1}$ D-mannitol. The flasks were incubated at 30 °C for 4 days in a static incubator. The as-prepared cellulose was dipped into 1 wt% NaOH at 80 °C to remove remaining bacterial and culture liquid, and subsequently washed several times until neutral pH. The AgNWs synthesis procedure was as follows: 100 mL EG was heated at 170 °C for 1 h in oil-bath pan to remove water. ~ 0.2 g PVP as stabilizer, 0.17 g $AgNO_3$, and 2.4 mg $CuCl_2$ were all dispersed into 60 ml EG in hotplate by stirring for 30 min to ensure uniform dispersion. The mixture was added into a 100 ml beaker and heated at 145 °C for 6 h in oil-bath pan. The precipitate was centrifuged three times under 1000 rpm for 3 min with acetone and centrifuged three times to obtain AgNWs in ethyl alcohol. Lastly, under the condition of optimum ratio, 10.8 mg AgNWs was dispersed into 200 mL ethyl alcohol and filtered on the as-prepared single-sided BC matrix, as shown in Scheme 1.

### Measurement and characterization

The morphologies and microstructure of these samples were characterized by scanning electron microscope (SEM; Hitachi S4800), transmission electron microscope (TEM/HRTEM; JEOL-2100) and X-ray diffraction (XRD; X'Pert Pro MPD). The elemental composition of the obtained BC/AgNWs films was analyzed by X-ray photoelectron spectroscopy (XPS, Escalab 250Xi, Thermo Scientific Escalab, USA). The conductivity of the sample was tested by a four-point probe (Baishen Technology, China). The optical transmittance was measured by ultraviolet–visible spectroscope (UV-3600, SHIMADZU). An uniaxial testing machine (INSTRON1185, Instron

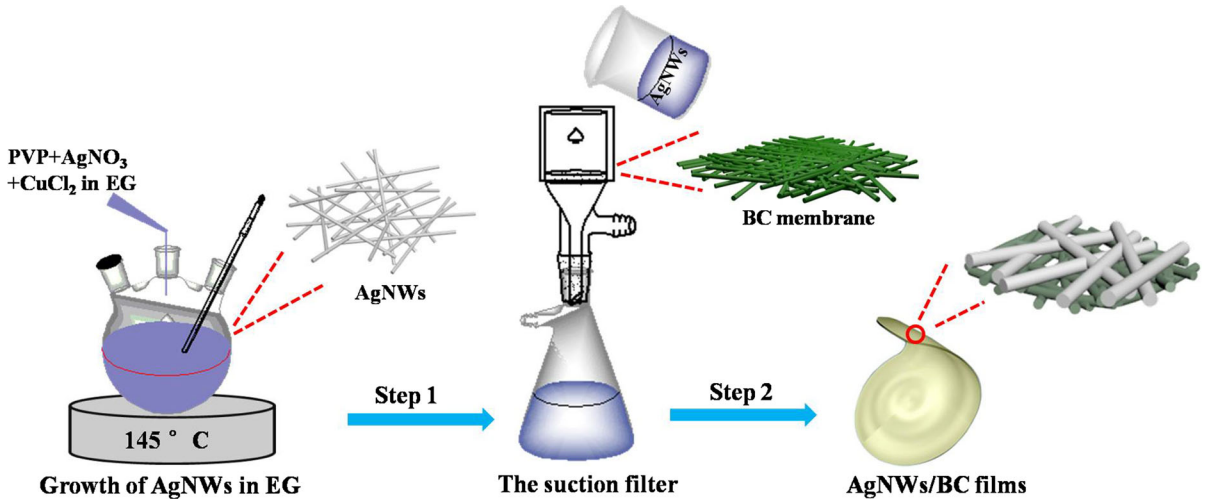


**Scheme 1** Schematic dagram of synthesis of AgNWs/BC composite films (not to scale)

Corporation, USA) was used to test the mechanical properties of the samples, and an average value was calculated by ten reduplicative tests of each sample of 1 cm in width, 5 cm in length.

## Results and discussion

### Morphology analyses

Figure 1a, b shows the SEM images of the as-prepared BC and BC/AgNWs composite films. Figure 1a shows the width of BC ranges from 10 to 70 nm with an average width of 30 nm. The BC nanofibers formed a highly ultrafine porous network stabilized by extensive hydrogen bonding that lead to its character as a highly flexible and mechanically robust system (Feng et al. 2012). Figure 1b reveals AgNWs have been synthesized and no other impurities could be detected. As shown in the inset Fig. 1b (top right), the width of AgNWs varied from 180 to 210 nm with an average width of 196 nm and length of 150 μm (Fig. 1d). Thus, a high aspect ratio of the AgNWs materials was calculated ($\sim$ 1000) which is superior to what has been previously reported (Xu and Zhu 2012; Yu et al. 2017). Figure 1c reveals interface between AgNWs and BC matrix, suggesting AgNWs tightly attached to the surface of BC matrix. Figure 1e provides a TEM image of the as-prepared AgNWs that demonstrates a smooth and flat surface. Such results imply that the applicability of AgNWs as flexible transparent electrodes and potentially wearable/implantable devices is very high. The thickness of composite thin films is close to 98.8 $\pm$ 0.44 nm, as presented in Fig. 1f.

### XRD and TEM analysis

The XRD pattern shown in Fig. 2a proves the presence of the AgNWs in the films. Typical diffraction peaks at $2\theta$ of 14.5° and 22.6° can be assigned to (100) and (110) of the crystallographic planes of BC, which mostly has the Iα allomorph (French 2014; Lv et al. 2016). The substantial variations in peak intensities from ideal patterns for Iα (French 2014) can be attributed to preferred orientation of the crystallites in the films. Additionally, the significant diffraction peaks at $2\theta$ of 38.3°, 44.32°,65.54° and 77.40° correspond to the (111), (200), (220) and (311) planes of pure face-centered-cubic silver crystals, respectively (JCPDS file No. 04-0783). No impurities were detected, implying the formation of highly pure silver. Figure 2b reveals a typical TEM image of an individual AgNW that is 195 nm in diameter with a d spacing of 0.286 nm corresponding to the (111) plane of silver crystals.

### XPS analysis

XPS further supports the characterization of the elements and structure of BC/AgNWs films shown in Fig. 3. Figure 3a illustrates five crucial peaks at

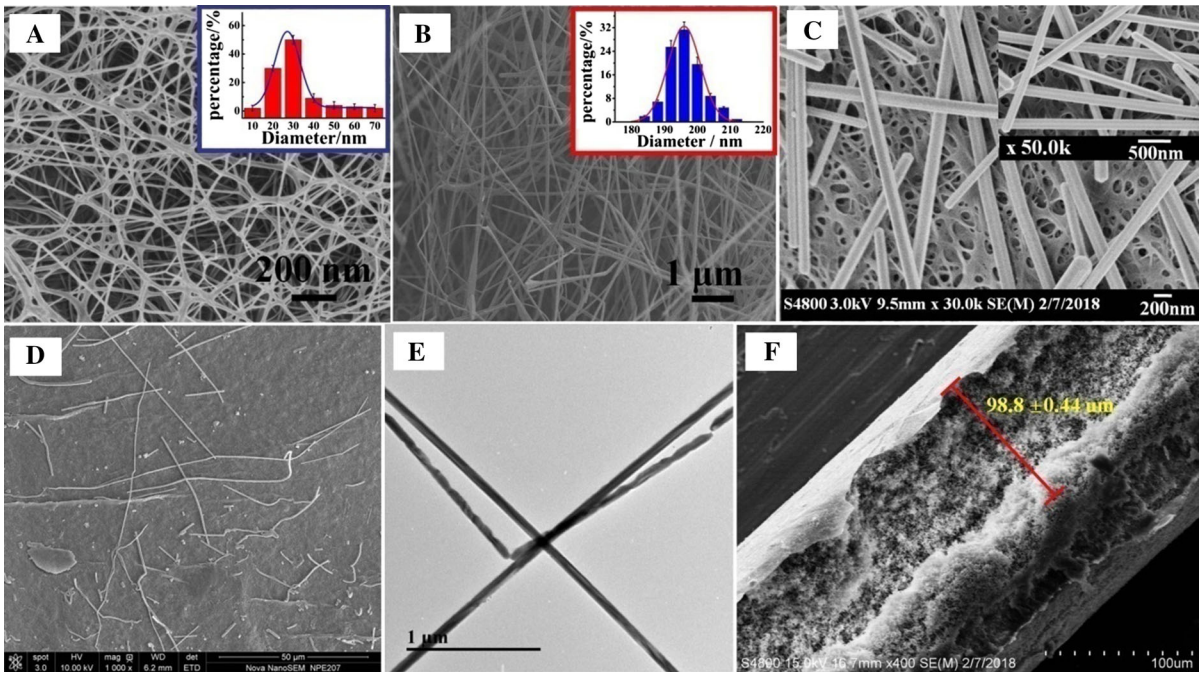


**Fig. 1** **a**, **b** FE-SEM images of as-prepared samples: BC and BC/AgNWs composite films; **c** FE-SEM image of interface between AgNWs and BC matrix, corresponding the top right inset presents FE-SEM of AgNWs-attached BC matrix (enlarged); **d** FE-SEM image of as-synthesized AgNWs (enlarged); corresponding TEM of **e** AgNWs, respectively; SEM image of cross sections of **f** BC/AgNWs composite films

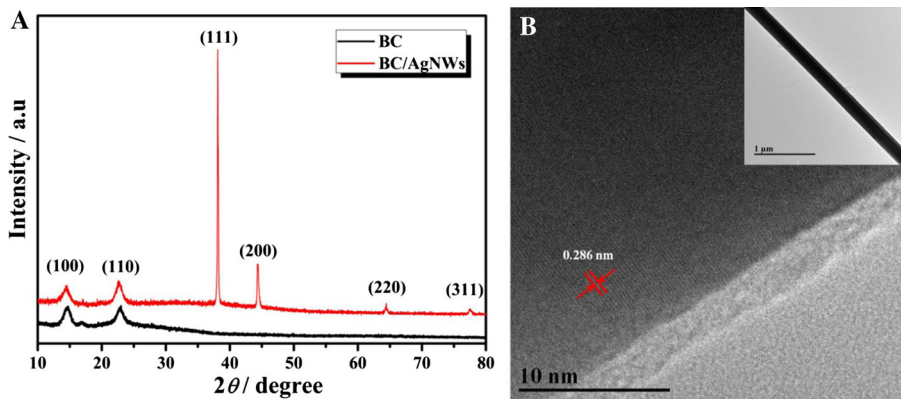


**Fig. 2** **a** XRD pattern of as-prepared BC and BC/AgNWs; **b** HRTEM of the AgNWs, corresponding the top right inset has TEM of an individual AgNW

608, 584, 532, 378, and 285 eV corresponding to the binding energies of Ag $3p_{1/2}$, Ag $3p_{3/2}$, O1 s, Ag3d, and C1 s (Oytun et al. 2017; Wan and Li 2016; Zheng et al. 2003), respectively. The as-prepared sample is mainly composed of C, O, and Ag. The high-resolution spectrum of Ag 3d further confirms the presence of two peaks at 373.88 and 367.68 eV, which can be assigned to Ag $3d_{3/2}$ and Ag $3d_{5/2}$ of metallic silver (Cheng et al. 2010), respectively, as illustrated in Fig. 3b. Thus, XRD and XPS results indicate that AgNWs have been successful synthesized and attached onto the BC matrix.

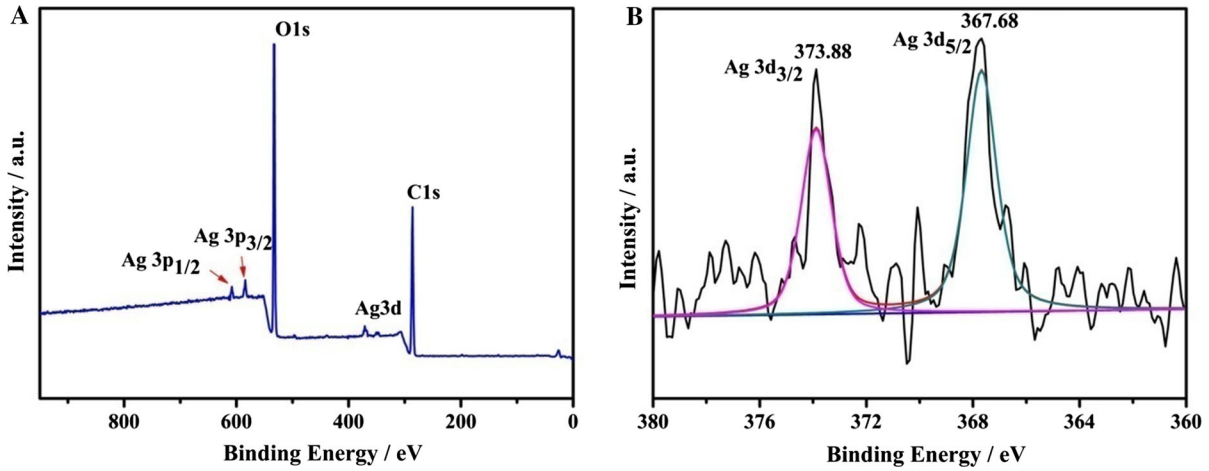


**Fig. 3** **a** XPS spectrum of as-prepared BC/AgNWs films and corresponding high-resolution Ag peaks of the films

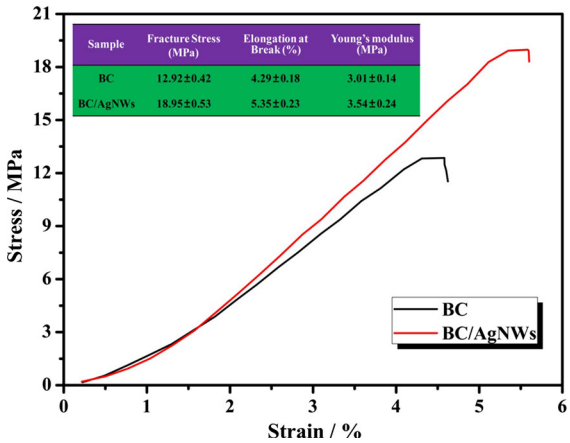


**Fig. 4** Tensile stress–strain curves of pure BC, BC/AgNWs films and corresponding the fracture stress, elongation at break and Young's modulus of as-prepared samples

## Mechanical properties

Typical tensile stress–strain (TS) curves were evaluated by TS and elongation at break (EB). Figure 4 clearly displays that as-prepared samples showed a linear elastic behavior at the first stage until reaching to the yield point, and then until the samples were broken, due to the individual fibers and nano-layers were slipped and pulled out along the stretching direction. The data reveals the TS and EB value of the pure BC were about $12.92 \pm 0.42$ MPa and $4.29 \pm 0.18\%$, respectively. The as-synthesized AgNWs on BC membrane increased of its corresponding values as compared to pure BC which nearly $18.95 \pm 0.53$ MPa of its fracture stress at EB ($5.35 \pm 0.23\%$). Thus, BC/AgNWs nanocomposites films shows a higher TS and EB a finding that could be attributed to two mechanisms. Firstly, some fibrils could be appear fracture and slippage in the process of pulling, and while concomitantly part breakage of AgNWs nano-layers may be occur under some external force. Meanwhile, by comparison with BC, the Young's modulus value for BC/AgNWs films was $3.54 \pm 0.24$ MPa as shown in the inset of Fig. 4. In general, BC/AgNWs exhibited the best tolerance across a broader mechanical strength, making it a desirable material for many practical areas.

## Optical and electrical properties

Figure 5a reveals that pure BC membranes exhibit excellent transparency with transmittance values of 88.4% at 550 nm and 89.1% at 700 nm in the UV–Vis region. However, as-prepared BC/AgNWs films, as compared to pure BC membrane display a slight diminution, although still very acceptable, in transparency of 79.1% at 550 nm and 80.1% at 700 nm, respectively. Figure 5b reveals virtual transparency for pure BC. Compared with Fig. 5b, AgNWs-attached BC films has very little change detected by the naked eye, as noted (Fig. 5c) by the University Logo (Jiangnan) displaying very clearly. To demonstrate the effect of bent states on conductivity, the sample was tested in flat and bent states at angle of various degrees shown in Fig. 5d. The conductivities were tested at the central regions of the films to reveal resistances from

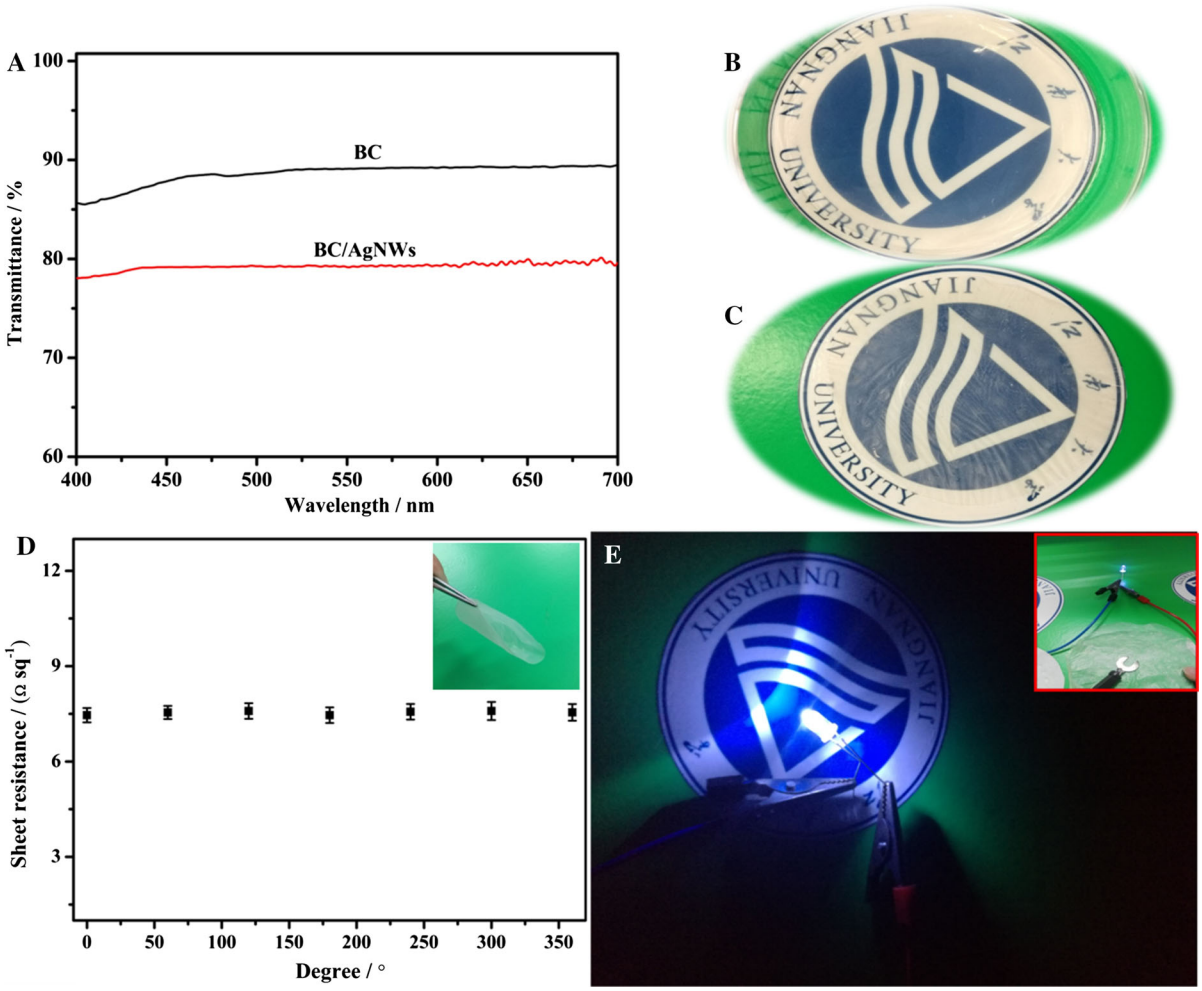


**Fig. 5** Photographic images of **a** BC and **b** BC-based AgNWs films; **c** light transmittance of the films from 400 to 700 nm; **d** the effect of bent states on the conductivity of BC/AgNWs nanocomposites at different degrees (°): 0; 60; 120; 180; 210; 240; 300; and 360; **e** photographic image of the transparent film

$7.46 \pm 0.22\ \Omega\ sq^{-1}$ at bending angles of approximately 0°, to $7.55 \pm 0.26\ \Omega\ sq^{-1}$ at a bending angle of approximately 0°. Meanwhile, to demonstrate the toughness-enabled flexibility, the films were bent until the ends contacted each other as shown in the inset of Fig. 5d. The results showed the conductivity of bent states of the obtained films were unchanged, a finding that points to stability of the junction of BC and AgNWs. Figure 5e reveals that the as-prepared films were endowed with excellent conductive performance.

## Conclusions

Herein, AgNWs were synthesized via a simple and rapid one-step method that not only provided materials with high aspect ratios, but also exhibited high transparency. The as-prepared BC/AgNWs films possessed low sheet resistance, good mechanical strength, satisfactory optical properties, and excellent flexibility. Thus, green, easily prepared, and flexible BC-based transparent composites films were successful fabricated that may have significant potential for transparent conductive applications.

**Acknowledgments** This research was financially supported by the National Natural Science Foundation of China (51641303), the 111 Project (B17021), the Priority Academic Program Development of Jiangsu Higher Education Institutions, The State Scholarship Fund from China Scholarship Council (201706790088), the Natural Science Foundation of Jiangsu Province (BK20150155), the Innovation Program for Graduate Education in Jiangsu Province (KYLX16_0794) and (KYCX17_1437), the Fundamental Research Funds for the Central Universities (JUSRP51621A and JUSRP11701).

## References

Bade SG, Li J, Shan X, Ling Y, Tian Y, Dilbeck T, Besara T, Geske T, Gao H, Ma B (2016) Fully printed halide perovskite light-emitting diodes with silver nanowire electrodes. ACS Nano 10:1795–1801

Bobinger M, Mock J, Torraca PL, Becherer M, Lugli P, Larcher L (2017) Tailoring the aqueous synthesis and deposition of copper nanowires for transparent electrodes and heaters. Adv Mater Interf. https://doi.org/10.1002/admi.201700568

Celle C, Mayousse C, Moreau E, Basti H, Carella A, Simonato JP (2012) Highly flexible transparent film heaters based on random networks of silver nanowires. Nano Res 5:427–433

Cheng B, Le Y, Yu J (2010) Preparation and enhanced photocatalytic activity of Ag@$TiO_2$ core-shell nanocomposite nanowires. J Hazard Mater 177:971–977

Dong Y, Mallineni SSK, Maleski K, Behlow H, Mochalin VN, Rao AM, Gogotsi Y, Podila R (2018) Metallic MXenes: a new family of materials for flexible triboelectric nanogenerators. Nano Energy 44:103–110

Ellmer K (2012) Past achievements and future challenges in the development of optically transparent electrodes. Nat Photonics 6:809–817

Fabra MJ, López-Rubio A, Ambrosio-Martín J, Lagaron JM (2016) Improving the barrier properties of thermoplastic corn starch-based films containing bacterial cellulose nanowhiskers by means of PHA electrospun coatings of interest in food packaging. Food Hydrocoll 61:261–268

Feng Y, Zhang X, Shen Y, Yoshino K, Feng W (2012) A mechanically strong, flexible and conductive film based on bacterial cellulose/graphene nanocomposite. Carbohyd Polym 87:644–649

French AD (2014) Idealized powder diffraction patterns for cellulose polymorphs. Cellulose 21:885–896

Hecht DS, Hu L, Irvin G (2011) Emerging transparent electrodes based on thin films of carbon nanotubes, graphene, and metallic nanostructures. Adv Mater 23:1482–1513

Hu W, Chen S, Zhou B, Liu L, Ding B, Wang H (2011) Highly stable and sensitive humidity sensors based on quartz crystal microbalance coated with bacterial cellulose membrane. Sensor Actuat B-Chem 159:301–306

Kim T, Canlier A, Kim GH, Choi J, Park M, Han SM (2013) Electrostatic spray deposition of highly transparent silver nanowire electrode on flexible substrate. Acs Appl Mater Inter 5:788–794

Lin H, Li L, Ren J, Cai Z, Qiu L, Yang Z, Peng H (2013) Conducting polymer composite film incorporated with aligned carbon nanotubes for transparent, flexible and efficient supercapacitor. Sci Rep 3:1353–1358

Liu Y, Zhang J, Gao H, Wang Y, Liu Q, Huang S, Guo CF, Ren Z (2017) Capillary-force-induced cold welding in silver-nanowire-based flexible transparent electrodes. Nano Let 17:1090–1096

Lu P, Cheng F, Ou Y, Lin M, Su L, Chen S, Yao X, Liu D, Lu P, Cheng F (2017) A flexible and transparent thin film heater based on a carbon fiber/heat-resistant cellulose composite. Compos Sci Technol. https://doi.org/10.1016/j.compscitech.2017.09.033

Lv P, Wei A, Wang Y, Li D, Zhang J, Lucia LA, Wei Q (2016) Copper nanoparticles-sputtered bacterial cellulose nanocomposites displaying enhanced electromagnetic shielding, thermal, conduction, and mechanical properties. Cellulose 23:1–11

Lv P, Yao Y, Li D, Zhou H, Naeem MA, Feng Q, Huang J, Cai Y, Wei Q (2017) Self-assembly of nitrogen-attached carbon dots anchored on bacterial cellulose and their application in iron ion detection. Carbohyd Polym 172:93–101

Oytun F, Kara V, Alpturk O, Basarir F (2017) Fabrication of solution-processable, highly transparent and conductive electrodes via layer-by-layer assembly of functional silver nanowires. Thin Solid Films 636:40–47

Peng S, Fan L, Wei C, Bao H, Zhang H, Xu W, Xu J (2016) Polypyrrole/nickel sulfide/bacterial cellulose nanofibrous composite membranes for flexible supercapacitor electrodes. Cellulose 23:2639–2651

Pinto ERP, Barud HS, Silva RR, Palmieri M, Polito WL, Calil VL, Cremona M, Ribeiro SJL, Messaddeq Y (2015) Transparent composites prepared from bacterial cellulose and castor oil based polyurethane as substrates for flexible OLEDs. J Mater Chem C 3:11581–11588

Qiu Y, Qiu L, Cui J, Wei Q (2016) Bacterial cellulose and bacterial cellulose-vaccarin membranes for wound healing. Mater Sci Eng C Mater Biol Appl 59:303–309

Ramani D, Sastry TP (2014) Bacterial cellulose-reinforced hydroxyapatite functionalized graphene oxide: a potential osteoinductive composite. Cellulose 21:3585–3595

Schumann DA, Wippermann J, Klemm DO, Kramer F, Koth D, Kosmehl H, Wahlers T, Salehi-Gelani S (2009) Artificial vascular implants from bacterial cellulose: preliminary results of small arterial substitutes. Cellulose 16:877–885

Sekitani T, Nakajima H, Maeda H, Fukushima T, Aida T, Hata K, Someya T (2009) Stretchable active-matrix organic light-emitting diode display using printable elastic conductors. Nat Mater 8:494–499

Thiruvengadam V, Vitta S (2017) Bacterial cellulose based flexible multifunctional nanocomposite sheets. Cellulose 24:3341–3351

Trovatti E, Carvalho AJ, Ribeiro SJ, Gandini A (2013) Simple green approach to reinforce natural rubber with bacterial cellulose nanofibers. Biomacromol 14:2667–2674

Ullah H, Santos HA, Khan T (2016) Applications of bacterial cellulose in food, cosmetics and drug delivery. Cellulose 23(4):2291–2314

Wan C, Li J (2016) Cellulose aerogels functionalized with polypyrrole and silver nanoparticles: in-situ synthesis, characterization and antibacterial activity. Carbohyd Polym 146:362–367

Wang B, Li X, Luo B, Yang J, Wang X, Song Q, Chen S, Zhi L (2013) Pyrolyzed bacterial cellulose: a versatile support for lithium ion battery anode materials. Small 9:2399–2404

Wu CN, Cheng KC (2016) Strong, thermal-stable, flexible, and transparent films by self-assembled TEMPO-oxidized bacterial cellulose nanofibers. Cellulose 24:1–15

Wu F, Li Z, Ye F, Zhao X, Zhang T, Yang X (2016) Aligned silver nanowires as transparent conductive electrodes for flexible optoelectronic devices. J Mater Chem C 4:11074–11080. https://doi.org/10.1039/c6tc03671f

Wu H, Williams GR, Wu J, Wu J, Niu S, Li H, Wang H, Zhu L (2018) Regenerated chitin fibers reinforced with bacterial cellulose nanocrystals as suture biomaterials. Carbohyd Polym 180:304–313

Xu F, Zhu Y (2012) Highly conductive and stretchable silver nanowire conductors. Adv Mater 24:5117–5122

Yu X, Yu X, Zhang J, Chen L, Long Y, Zhang D (2017) Optical properties of conductive silver-nanowire films with different nanowire lengths. Nano Res 11:3706–3714

Zeng XY, Zhang QK, Yu RM, Lu CZ (2010) A new transparent conductor: silver nanowire film buried at the surface of a transparent polymer. Adv Mater 22:4484–4488

Zhang Y, Guo J, Xu D, Sun Y, Yan F (2017) One-pot synthesis and purification of ultra-long silver nanowires for flexible transparent conductive electrodes. Acs Appl Mater Int 9:25465–25473

Zheng X, Zhu L, Yan A, Wang X, Xie Y (2003) Controlling synthesis of silver nanowires and dendrites in mixed surfactant solutions. J Colloid Interf Sci 268:357–361